Supplementary Materials

Crystal Facet Engineering of Pt_1/Co_3O_4 Single-Atom Catalysts for Highly Selective Hydrogenation of Cinnamaldehyde

Liyun Huang[‡a,b], Zheng Zhang[‡a], Qingdi Sun[a], Huanshi Lan[c], Liangbin Wang[d,*], Xiaohui He[a,*]

EXPERIMENTAL

1. Materials

$Co(NO_3)_2 \cdot 6H_2O$, NaOH, HOOCCOOH, $Na_2C_2O_4$, $NH_3 \cdot H_2O$, cinnamaldehyde (CAL), cinnamyl alcohol (COL), hydrocinnamaldehyde (HCAL), cinnamyl alcohol, ethyl alcohol and tridecane were purchased from Shanghai Aladdin Biochemistry Technology Co. Ltd, China. All chemical and materials were used as received without any further purification. Deionized water was used throughout this work.

2. Catalyst Preparation

Co_3O_4 with cubic (Co_3O_4-c), truncated octahedral (Co_3O_4-t), and octahedral (Co_3O_4-o) morphologies were synthesized via a hydrothermal method. For Co_3O_4-c, 0.4 g NaOH and 11.6 g $Co(NO_3)_2 \cdot 6H_2O$ were dissolved in 40 mL deionized water, transferred to a 100 mL Teflon-lined autoclave, and heated at 180 °C for 5 h. Co_3O_4-t was obtained by dissolving 1.7 g oxalic acid, 2.0 g NaOH, and 24.7 g $Co(NO_3)_2 \cdot 6H_2O$ in 70 mL deionized water, followed by hydrothermal treatment at 220 °C for 20 h. Similarly, Co_3O_4-o was prepared using 2.0 g sodium oxalate, 0.8 g NaOH, and 24.7 g $Co(NO_3)_2 \cdot 6H_2O$ in 70 mL deionized water, maintained at 220 °C for 20 h. After cooling, the precipitates were collected, washed with ethanol and deionized water, dried at 60 °C for 5 h, and calcined at 500 °C for 3 h.

Pt_1/Co_3O_4 catalysts were synthesized via impregnation. Co_3O_4 (c, t, or o) was dispersed in a $Pt(NH_3)_4(NO_3)_2$ solution (0.2 wt% Pt), and the pH was adjusted to 8 with diluted ammonia. The mixture was stirred in a 50 °C water bath for 3 h, followed by centrifugation and washing. The obtained precipitate was dried at 60 °C for 5 h and calcined at 400 °C for 2 h to yield Pt_1/Co_3O_4 catalysts.

3. Catalytic Performance Evaluation

Selective hydrogenation of cinnamaldehyde was performed in a 10 mL stainless-steel autoclave reactor. A typical reaction involved adding 0.1 mmol CAL, 10 mg catalyst, 2 mL

ethanol, and tridecane (internal standard) to the reactor. The system was purged with H_2 (5 times) to remove air, followed by reaction at 40 °C under 0.5 MPa H_2 for 25 h.

Reaction products were analyzed using gas chromatography (GC) (Shimadzu GC-2010 Plus) equipped with an InertCap Pure-WAX capillary column (30 m × 0.25 mm) and a flame ionization detector (FID). The chemical identity of the products was confirmed via gas chromatography-mass spectrometry (GC-MS) (Shimadzu). The catalyst's reusability was assessed by separating the used catalyst via centrifugation, washing with ethanol, and reusing it under identical conditions.

4. Catalyst characterization

The morphology and structure of the catalysts were examined using field-emission scanning electron microscopy (FE-SEM) (Zeiss Gemini 500) and transmission electron microscopy (TEM) (FEI Tecnai G2 F30, 300 kV). Aberration-corrected high-angle annular dark-field scanning transmission electron microscopy (AC HAADF-STEM) and energy-dispersive spectroscopy (EDS) mapping were conducted on a JEM-ARM200F microscope (200 kV) to analyze the dispersion of Pt atoms. X-ray diffraction (XRD) patterns were recorded on a Bruker D8 Advanced diffractometer with Cu Kα radiation (λ = 1.5406 Å) at a scan rate of 5°/min over a 2θ range of 10–80°. X-ray absorption spectroscopy (XAS) measurements at the Pt L_3-edge were carried out at beamline BL14W of the Shanghai Synchrotron Radiation Facility (SSRF). The oxidation state and electronic properties of Pt were analyzed using X-ray photoelectron spectroscopy (XPS) (Thermo ESCALAB250), with the C 1s peak at 284.6 eV as the reference. The Brunauer-Emmett-Teller (BET) method was applied to determine the surface area and porosity of the catalysts using a Micromeritics ASAP 2020M analyzer. The Pt loading was measured using inductively coupled plasma mass spectrometry (ICP-MS) (Agilent-7700). Fourier-transform infrared spectroscopy (FTIR) was performed using a Nicolet iS20 spectrometer in the 400–4000 cm^{-1} range. H_2-temperature-programmed reduction (H_2-TPR) was carried out on an AutoChem II 2920 system, and in situ diffuse reflectance infrared Fourier-transform spectroscopy (in situ DRIFTS) was conducted on a Thermo Nicolet iS50 instrument. In H_2-D_2 exchange experiments, catalyst powders (~15 mg) were placed in a quartz reactor, and the reaction was monitored using a Hiden Analytical HPR-20 QIC mass spectrometer.

5. DFT Calculation Methods and Parameter Settings

Density functional theory (DFT) calculations were performed using the slab model in the Vienna ab-initio simulation package (VASP), with the Perdew-Burke-Ernzerhof (PBE) method (within the Generalized Gradient Approximation (GGA) framework) and the Projector Augmented Wave (PAW) method employed. For geometry optimization and adsorption energy calculations, the Monkhorst-Pack method was used to select 2×2×1 and 6×6×1 k-point grids. The energy cutoff for the plane-wave expansion of electronic wavefunctions was set to 400 eV; the convergence thresholds for energy and electron density were 10-4 eV; the force threshold for atoms was 0.05 eV/Å; and the vacuum layer thickness was 15 Å. The adsorption energy (E_{ad}) is defined as:$E_{ad}=E_{total}-E_g-E_{slab}$, where E_{total} refers to the energy of the adsorption system, E_g is the energy of the gaseous substrate, and E_{slab} represents the energy of the ideal surface.

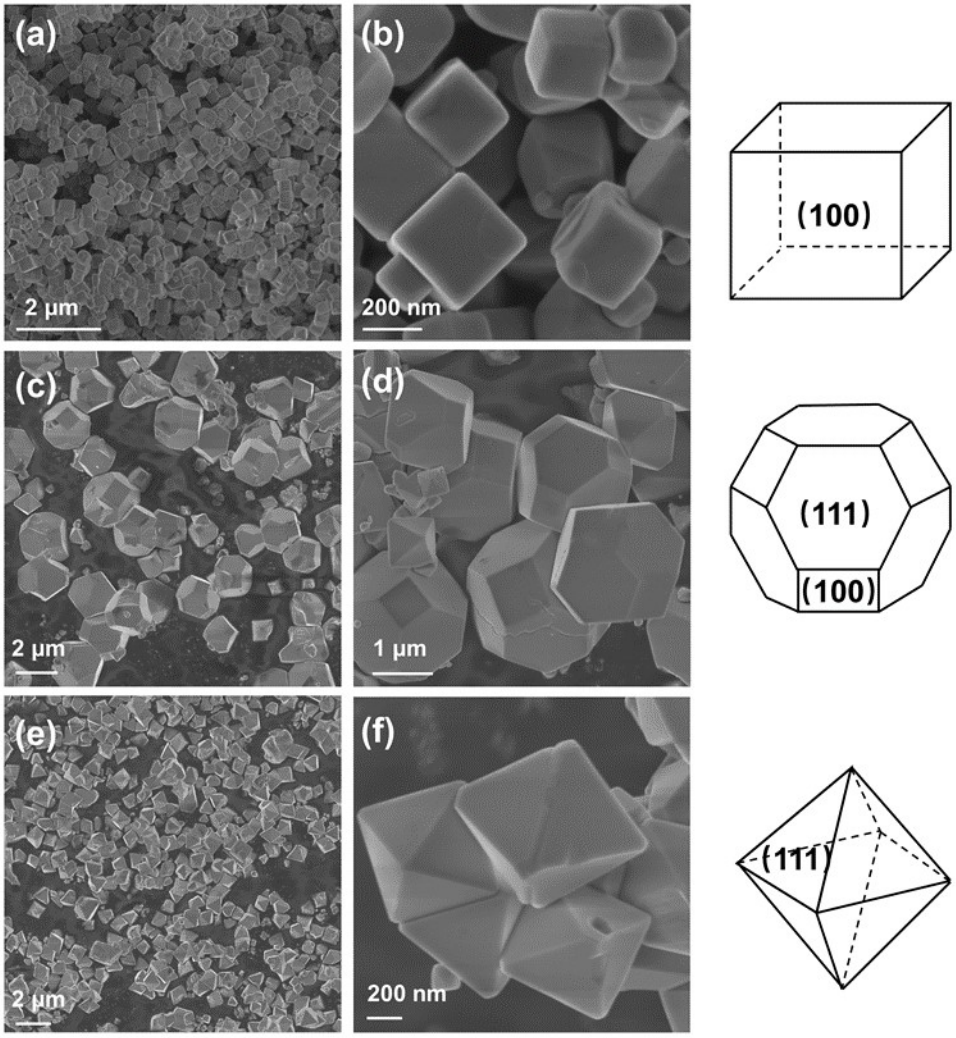

Figure S1. SEM images of (a, b) Co_3O_4-c, (c, d) Co_3O_4-t and (e, f) Co_3O_4-o and their structure models

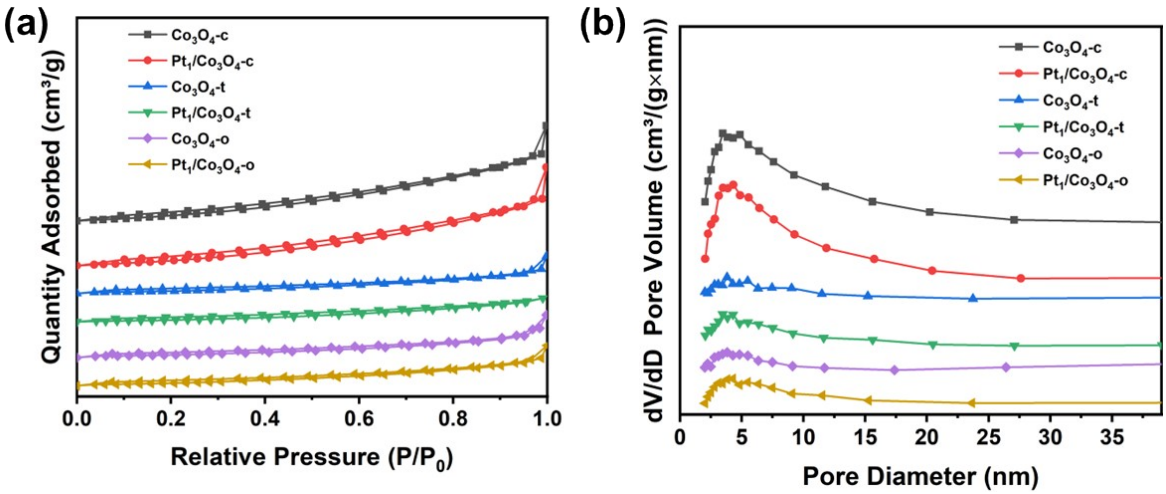

Figure S2. (a) N_2 adsorption-desorption isotherms and (b) pore size distribution of Co_3O_4-x (x = c, t, o) and Pt_1/Co_3O_4-x (x = c, t, o)

Table S1. Pt loadings and texture properties of various catalysts

Samples	Pt loading (wt%)	BET surface area (m^2/g)	Pore volume (cm^3/g)	Pore size (nm)
Co_3O_4-c	-	7.9	0.07	7.12
Co_3O_4-t	-	3.6	0.02	8.66
Co_3O_4-o	-	4.1	0.03	8.94
Pt_1/Co_3O_4-c	0.07	7.8	0.07	7.28
Pt_1/Co_3O_4-t	0.13	2.5	0.02	5.61
Pt_1/Co_3O_4-o	0.14	3.9	0.03	7.53

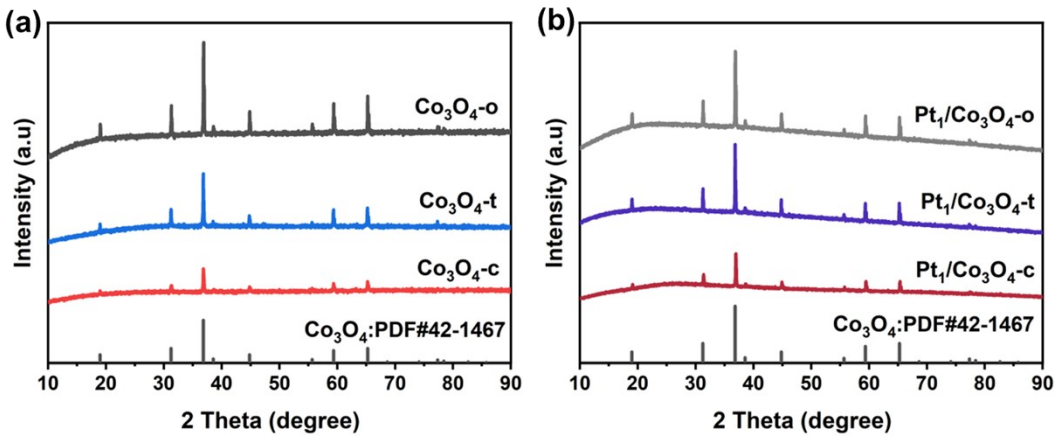

Figure S3. XRD patterns of (a) Co_3O_4-x (x = c, t, o) and (b) Pt_1/Co_3O_4-x (x = c, t, o)

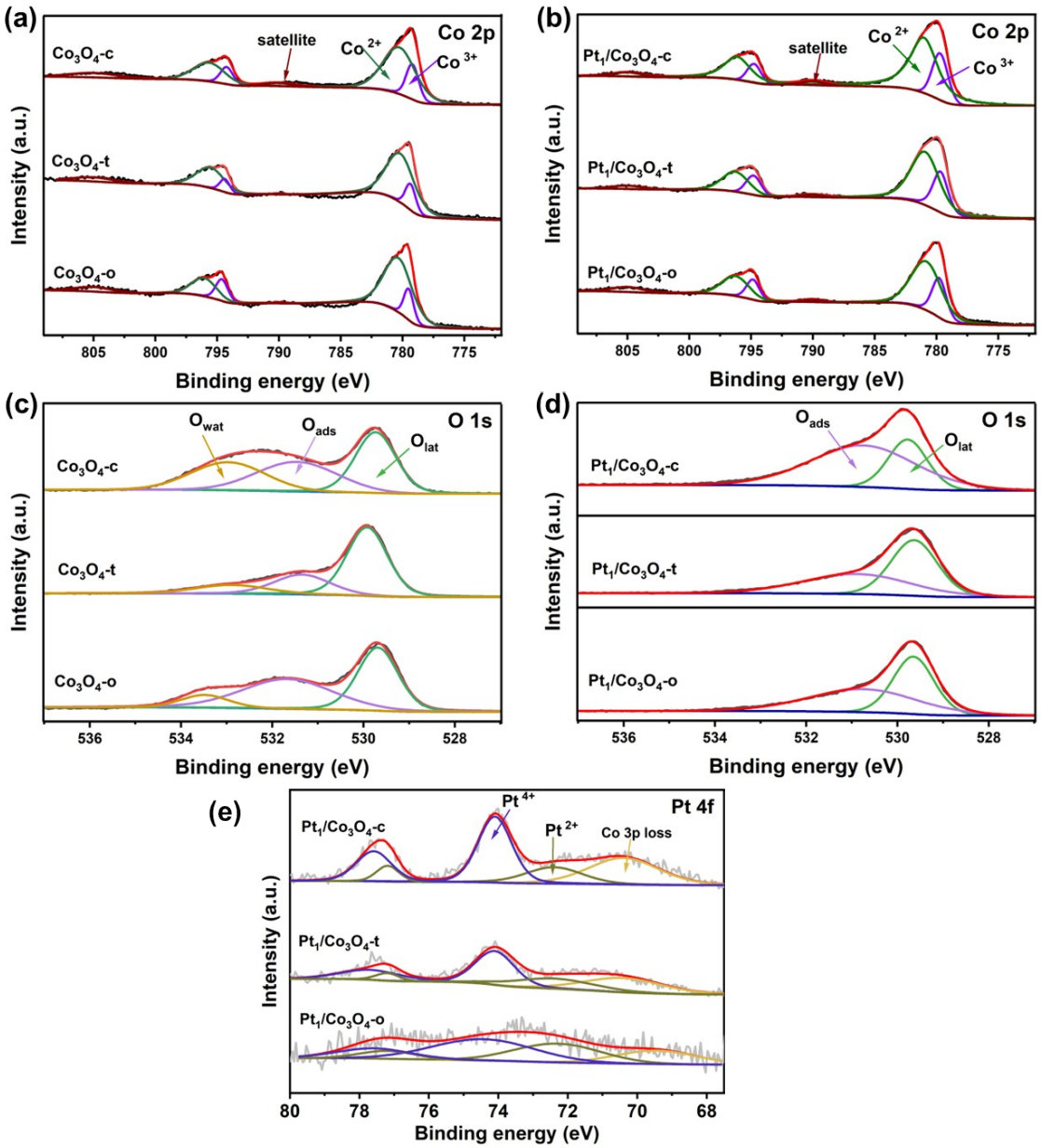

Figure S4. XPS spectra of Co 2p for (a) Co_3O_4-x (x = c, t, o) and (b) Pt_1/Co_3O_4-x (x = c, t, o), O 1s for (c) Co_3O_4-x (x = c, t, o) and (d) Pt_1/Co_3O_4-x (x = c, t, o), (d) Pt 4f for Pt1/Co3O4-x (x = c, t, o)

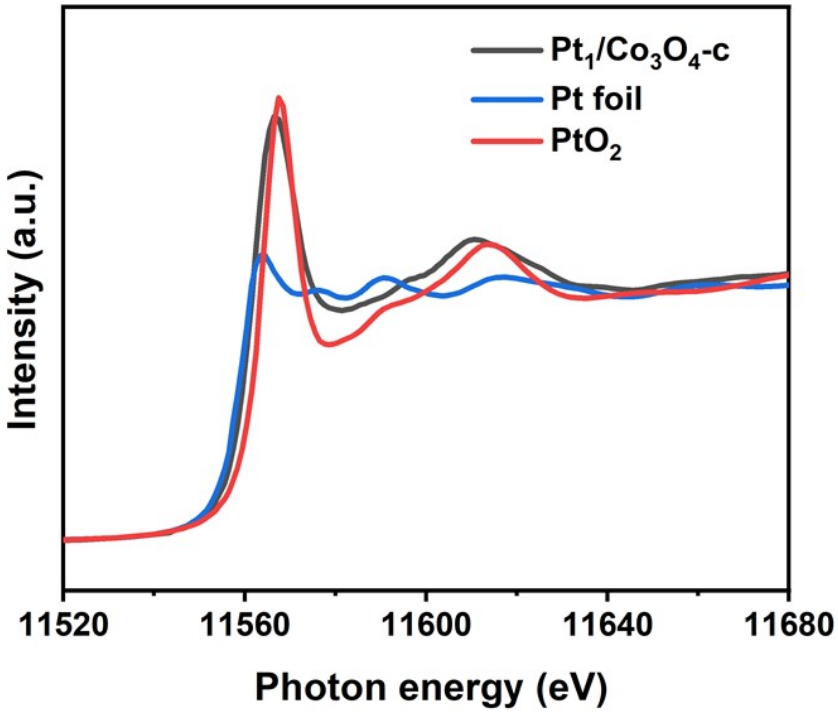

Figure S5. The normalized XANES spectra of Pt_1/Co_3O_4-c

Table S2. Structure parameters of EXAFS for Pt_1/Co_3O_4-c

Sample	Scattering path	CN[a]	R (Å)[b]	σ^2 ($\times10^{-3}$ Å^2)[c]	E_0 (eV)[d]
Pt_1/Co_3O_4-c	Pt-O	5.10±1.45	1.99±0.03	2.03±4.32	9.87±3.17

[a]CN is the coordination number; [b]R is bond distance; [c]σ^2 is Debye-waller factors; [d]E_0 is the inner potential correction. R–factor: 0.03.

Table S3. Specific activity analysis of Pt_1/Co_3O_4-x catalysts

Catalyst	loading (wt%)	Conversion rate (%)	TOF (h^{-1})	BET Surface Area (m^2/g)	Area-Normalized TOF ($h^{-1}\cdot g\cdot m^{-2}$)
Pt_1/Co_3O_4 -c	0.07	5.9	32.9	7.8	4.2
Pt_1/Co_3O_4 -t	0.13	12.1	7.3	2.5	2.9
Pt_1/Co_3O_4 -o	0.14	20.1	11.2	3.9	2.9

Note: It is noteworthy that Pt_1/Co_3O_4-o shows much lower TOF (11.2 h^{-1}) is than that of Pt_1/Co_3O_4-c (32.9 h^{-1}), indicating the superior intrinsic activity of Pt single atoms on the (100) facet. Additionally, the area-normalized TOF of Pt_1/Co_3O_4-c (4.2 $h^{-1}\cdot g\cdot m^{-2}$) is significantly higher than the other two samples, further confirming that the (100) facet of Co_3O_4 effectively modulates the catalytic activity of Pt single atoms.

Table S4. Weisz-Prater (WP) criterion calculation results for catalysts

Catalyst	r_{obs} (mol·g^{-1}·h^{-1})	R (cm)	WP Value	Conclusion
Pt_1/Co_3O_4-c	1.18×10^{-4}	1×10^{-5}	0.012	No internal diffusion limitation
Pt_1/Co_3O_4-t	4.84×10^{-5}	2.5×10^{-5}	0.031	No internal diffusion limitation
Pt_1/Co_3O_4-o	8.04×10^{-5}	3×10^{-5}	0.073	No internal diffusion limitation

Note: Kinetic Control Verification To confirm that the catalytic performance differences originate from the intrinsic activity of Pt single atoms (rather than mass transfer limitations), we systematically verified kinetic control by excluding external and internal diffusion effects. External diffusion, referring to the mass transfer of reactants from the solution to the catalyst surface, was eliminated by maintaining a constant and sufficient stirring speed throughout all experiments; this condition ensures catalyst particles are fully suspended (avoiding sedimentation or agglomeration) and reactants can rapidly reach the catalyst surface, minimizing liquid-solid mass transfer resistance, while consistent stirring intensity across experiments avoids variable interference from external diffusion. For the evaluation of internal diffusion limitations (mass transfer of reactants within catalyst pores), we employed the Weisz-Prater (WP) criterion, a quantitative tool widely used to distinguish kinetic control from internal diffusion control, with the core formula $WP = \frac{r_{obs} \times \rho_p \times R^2}{D_e \times C_0}$, with parameter definitions based on experimental facts and literature consensus: R (average carrier radius) is calculated from SEM images; r_{obs} (observed initial reaction rate) is derived from low-conversion data (5 h for Pt_1/Co_3O_4-c, 25 h for Pt_1/Co_3O_4-t and Pt_1/Co_3O_4-o) to avoid kinetic deviation; ρ_p=5.1 g cm^{-3} (bulk density of Co_3O_4); D_e=1×10^{-4} cm^2·h^{-1} (effective diffusion coefficient of cinnamaldehyde in mesopores); C_0=5×10^{-5} mol cm^{-3} (initial concentration of cinnamaldehyde).

Table S5. Adsorption energies (E_{ad}) of cinnamaldehyde (CAL) on Pt_1/Co_3O_4 surfaces

Catalyst surface	Adsorption configuration	Key interaction	E_{ad} (eV)
$Pt_1/Co_3O_4(100)$	Vertical (C=O bonded to Pt)	C=O-Pt interaction	-1.83
$Pt_1/Co_3O_4(100)$	Parallel (C=O + C=C bonded to Pt)	Dual C=O/C=C-Pt interaction	-0.43
$Pt_1/Co_3O_4(111)$	Vertical (C=O bonded to Pt)	C=O-Pt interaction	-2.08
$Pt_1/Co_3O_4(111)$	Parallel (C=O + C=C bonded to Pt)	Dual C=O/C=C-Pt interaction	-2.09

Table S6. A comparison of catalytic performance in CAL hydrogenation between our work and reported catalysts

Catalyst	Reaction conditions	Conversion rate (%)	Selectivity of cinnamyl alcohol	Ref.
Pt_1/Co_3O_4 -c	CAL 0.10 mmol; catalyst 10 mg; solvent EtOH 2 mL; H_2 0.5 MPa; 40 °C; 25 h	97.8	78.1	This work
Pd/oCNT	CAL 0.1 M in 1,4-dioxane; H_2 3 bar; 30 °C; WHSV 0.012 s^{-1}	85.8	93.5	[1]
Pt–Cu/SiO_2	Catalyst 50 mg；CAL 1.00 g（≈ 7.6 mmol）；*i*-PrOH 30 mL；H_2 10 bar；80 °C；2 h	37.9	64.1	[2]
Pt/TiO_2	CAL 0.1 mL in 4 mL of ethanol, 0.4mL of H_2O; catalyst 23 mg; H_2 2.0 MPa; 60 °C	92.6	95.4	[3]

[1] from *ACS Appl. Nano Mater.,* 2023, 6, 8868−8879.

[2] from *J. Chem.,* 2018, 1, 5608243.

[3] from *J. Phys. Chem. C,* 2021, 125, 13304−13312.